Measurement of hop moisture content and chromaticity during drying with VNIR hyperspectral imaging

Stuart Crichton [a,*], Jakob Münsterer[b], Klaus Kammhuber[c], Barbara Sturm[a,d]

[a] Postharvest Technologies and Processing Group, Department of Agricultural and Biosystems Engineering, University of Kassel, Witzenhausen, Germany

[b] Bavarian State Office for Agriculture, Hop Competence Centre Production Technologies, Wolnzach, Germany

[c] Bavarian State Office for Agriculture, Hop Research Centre Hüll, Wolnzach, Germany

[d] School of Agriculture, Food and Rural Development, Newcastle University, Newcastle upon Tyne, UK

* Corresponding author. Email: uk034880@uni-kassel.de

Abstract

With a single harvest a year the efficient processing of harvested hops is of great economic importance to growers. On top of this, the importance of drying immediately after harvest means that batches of hops should be dried in succession in an efficient manner in order to ensure both minimal product wastage and a consistent output quality level. Quality here refers to moisture content and colour of the dried hops. To investigate these during drying both a hyperspectral and a calibrated RGB camera were installed within a pilot scale dryer along with their illumination sources. During drying hops were imaged by both systems, while samples were removed for moisture content analysis. This enabled chemometric investigations into the prediction of moisture and chromatic information with a reduced wavelength set. Moisture content prediction was shown to be feasible (r^2=0.94, RMSE=0.27) for the test set using 8 wavelengths. CIELAB a* prediction was also seen to be feasible (r^2=0.75, RMSE=3.75), alongside CIELAB b* prediction (r^2=0.52 and RMSE=2.66). Future work to improve the current predictive models is also outlined.

Keywords: hop, drying, hyperspectral imaging, VNIR, moisture content, chromaticity

1. Introduction

The successful and efficient drying of hops, with one harvest a year, is of great economic importance to hop farmers. More so than other crops, hops are required to be dried immediately after harvesting to prevent any degradation in both colour and chemical content. This requirement for immediacy has led to farmers drying their hop harvest themselves on site and means they effectively need to be a jack-of-all-trades. This method of operation means that large amounts of hops are required to be dried in a very small timescale on site, and any method which can improve both the automation, efficiency of the process and the quality of the output product will be of great help.

To aid farmers in determining when hops have reached their desired moisture content currently temperature and humidity sensors are usually placed within the hop stack during drying. This method works well as a local (in spatial terms) non-destructive method to determine hop moisture content. However large variations in moisture content may exist within the overall hop stack, this method also ignores any potential monitoring of chromaticity change in the product. As such the potential for a method to non-destructively monitor chromaticity and moisture content over the entire hop stack could bring great benefits to the hop drying industry. Hyperspectral imaging (HSI) offers a potential single solution to investigate both chromaticity and chromatic changes in the hops continuously during drying (Pu & Sun, 2015; Wu et al., 2013; Wu, Shi, et al., 2012). The results presented here show the results of an investigation into the prediction of moisture content and chromaticity of hops.

2. Materials and Methods

All investigations were undertaken at the Research Station Hüll, Hallertau, Bavaria. The Mandarina hop variety was investigated, with all hops tested having been harvested immediately before drying (<60 minutes delay). A number of different drying conditions and hop bulk weights were tested. Three bulk weights of 12, 20 and 40kg/m^2 of hops were tested at three different process settings. These process settings were those of 1-3) 65°C air temperature with an air speed of 0.35m/s at each bulk weight, and 4) 70°C with an air speed of 0.35m/s with a bulk weight of 20kg. Each of these was replicated a total of 3 times. All tests were undertaken during the September 2015 harvest over 5 consecutive days to keep variations due to different ripeness as minimal as possible.

In order to carry out chromatic measurements a calibrated RGB camera was also placed within the dryer to monitor colour change, this was installed alongside the hyperspectral camera. This enabled hyperspectral measurements to be carried out at specific time points during drying and compared to captured colour data from the same time points. Hyperspectral images were captured at 0, 10, 20, 30, 40, 70, 100, 130 and 160 minutes for 20Kg at 65°C (Drying times were also varied for different conditions; up to 130 minutes for 70°C, and up to 220 minutes (190, 220) for 40Kg at

65°C) . In order to carry out the calibrated CIELAB capture correctly the halogen light source was turned off prior to RGB image capture (leaving only the 6500K fluorescent sources on). At these time points a portion (1600ml in volumetric terms) of the imaged samples (hyperspectral) were removed. A subset of this sample was utilised for moisture content analysis using the gravimetric weighing method.

Image capture at these set time intervals across the 4 different drying conditions led to the capture of 108 hyperspectral images and 108 corresponding calibrated RGB images. 2 hyperspectral images were subsequently discarded due to capture error, so all subsequent analysis was performed upon 106 images.

2.1. Imaging and drying set-up

To enable the imaging of hops during drying, within the dryer, a Specim V10E hyperspectral camera (Specim Spectral Imaging Ltd., Finland) was placed inside a protective casing within the dryer above the hop stack. The camera was used in combination with a mirror translation unit and a 35mm Schneider lens (Xenoplan 1.9/35, Schneider Optische Werke GmbH, Germany). Illumination was provided using a halogen security lamp fitted with a 500W halogen bulb, the lamp was attached on the interior wall of the dryer focused at the region directly beneath the camera system (Figure 1). The protective casing was constructed of steel, with an insulated lining. The casing also had a viewing window covered with a clear acrylic window sheet (Figure 1). This allowed the camera to view the hops situated directly below. This protective casing also provided ventilation to the camera during operation.

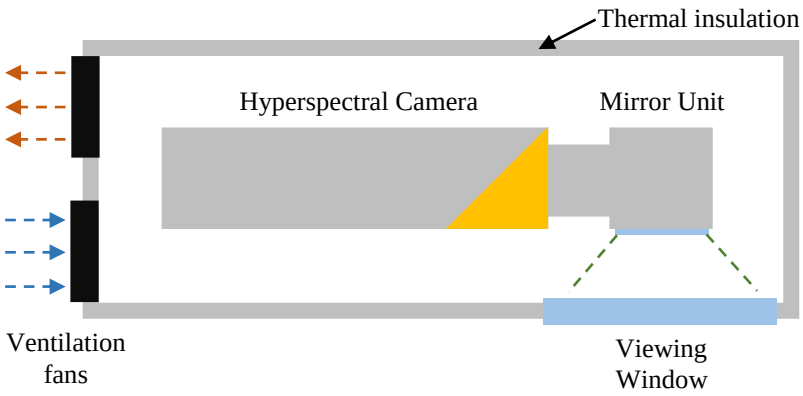

Figure 1. The design of the illumination and protective casing for the camera within the drying chamber.

This protective casing was attached to the interior of an experimental dryer above the top drying tray as outlined by Hofmann et al. (2013). This set up is shown in Figure 2 below.

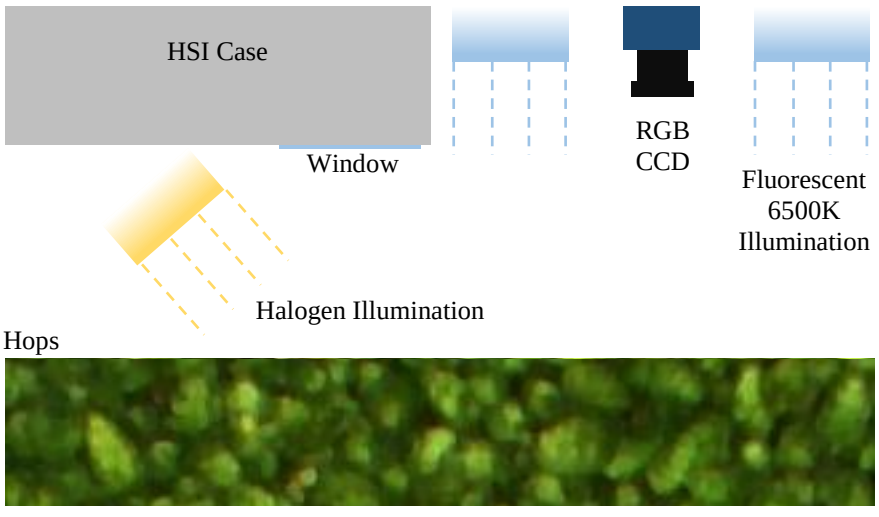

Figure 2. Location of imaging box in chamber, alongside CCD camera and illumination.

The lens was of a manual focus type and was focused at a specific hop depth, as such increasing blur did occur towards the lowest hop depths.

2.2. RGB imaging

In order to facilitate the chromatic measurement of hops during drying a RGB CCD camera was also positioned within the dryer, as shown previously in Figure 2. The system utilised a colour DFK 72AUC02-F (The Imaging Source, Germany) of resolution 1944*2592 (H*W). Illumination was provided by 2 Philips fluorescent light sources (Philips, Netherlands) of CCT 6500K and luminance of 2100 Lumens each.

2.3. RGB camera calibration

Color calibration of the RGB camera (The Imaging Source, Germany) was achieved through the polynomial color correction (Finlayson et al., 2015a). For calibration an X-Rite Color Checker Classic 24 patch chart (X-Rite Inc., Michigan, USA) was imaged using a set exposure in conjunction with a calibrated Q mini spectrophotometer (RGB Lasersystems, Germany). Polynomial color correction rather than root polynomial color correction (Finlayson et al., 2015b) was utilized due to the use of a single exposure for imaging during the drying process. Colourimteric data of each patch was then measured using a calibrated spectrometer (Q mini, RGB Photonics GmbH, Kelheim, Germany). The measured colorimetric XYZ values were then regressed alongside the measured average patch RGB values after subtraction of the average black patch RGB values. This produced a polynomial function which allowed the calculation of XYZ co-ordinates from measured RGB values. These calculated XYZ values were then converted into CIELAB co-ordinates using illuminant D65 as the reference white point, with a luminance value equal to the luminance of the white patch under the test illumination.

2.4. Hyperspectral Image Processing

Hyperspectral cubes were recorded using the Specim SpectralDAQ software (Specim Spectral Imaging Ltd., Finland), with all processing occurring within Matlab using software previously utilised in Crichton, Sturm, & Hurlbert (2015) and Crichton et al. (2016). Noise removal was carried out in the same manner presented in (Crichton et al., 2015).

However due to the nature of product shrinkage during drying conversion from irradiance to reflectance spectra involved the measurement of the incident illumination at a number of different heights and the resulting illumination field was smoothed with a small window operator to remove the influence of the non-perfectly uniform surface of the white reference tile. This height dependent illumination data was then utilised in combination with hop height measurements carried out at each sample period. Height dependent changes in the illumination field are shown in Figure 3.

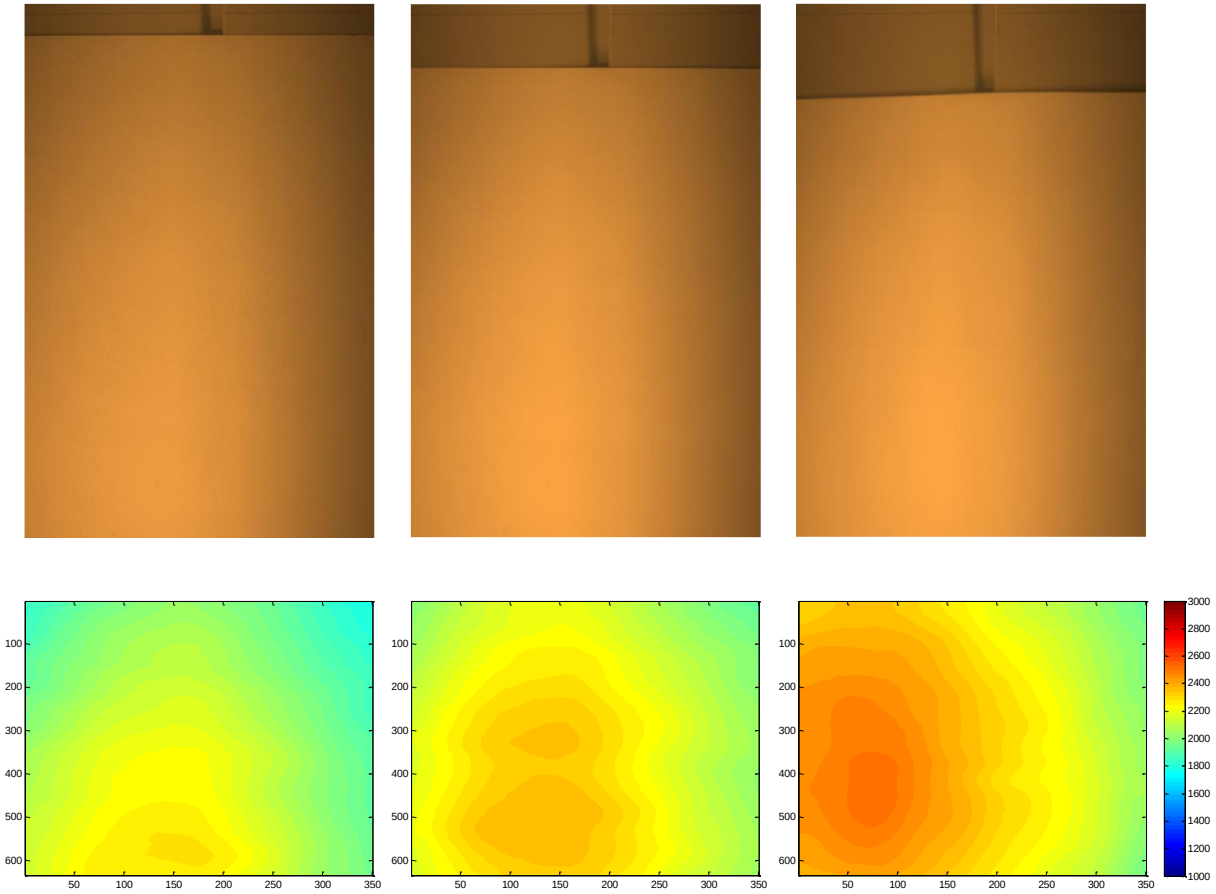

Figure 3. An illustration of how the intensity (at 669nm) and spatial distribution of illumination varies upon the hops as the hop height changes from a reference point at a) 5cm, b) 10cm and c) 15cm.

Images were then processed with the corresponding white reference image to produce the reflectance image on a pixel-by-pixel basis. Figure 4 illustrates the effect of conversion from irradiance to reflectance upon the calculated sRGB image from an example hyperspectral image.

Figure 4. Comparison between the sRGB image of the a) irradiance image, and b) the reflectance image.

However the nature of the hops being imaged and singular illumination direction led to challenges in image processing, which required further use of pre-processing methods. Both of these factors meant that when hops across the region of interest were analysed a great variation in spectral intensity existed. An example of this is shown below in Figure 5.

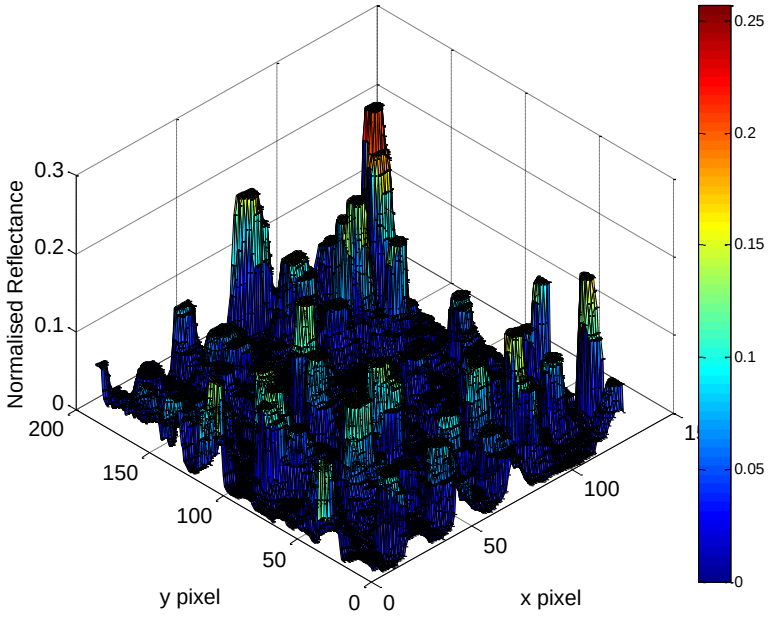

Figure 5. Illustration of the variation in the normalised reflectance for pixels at 669nm due to illumination geometry and hop distribution.

In order to counteract this, two different normalisation pre-processing methods (Amigo, Martí, & Gowen, 2013) were used; Normalisation and Standard Normal Variate (SNV). Using these two methods had the effect of minimising the baseline variation between pixels related to hop surface topology, as seen in Figure 6 below.

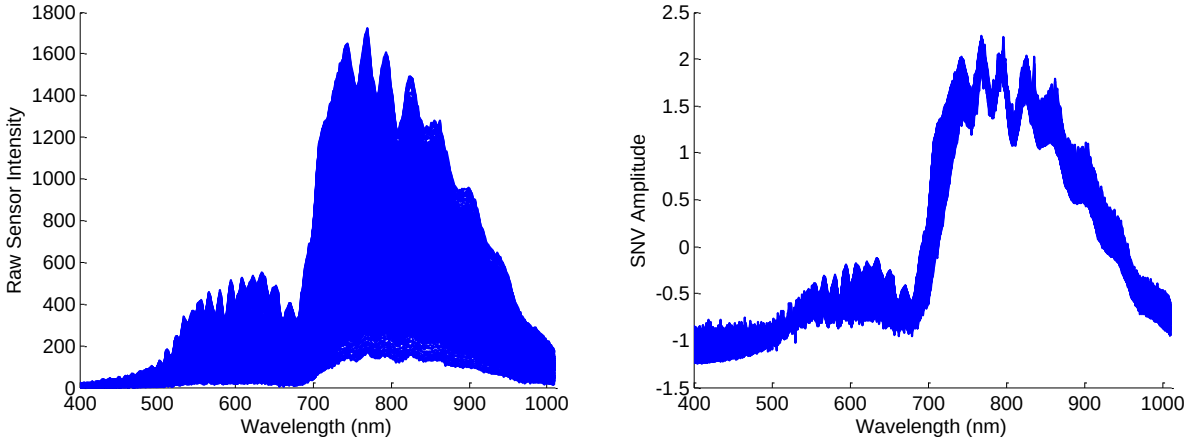

Figure 6. Illustrating the variation in irradiance due to the non-uniform topology of hops in a) the original image, and b) the effect of SNV pre-processing used to remove it.

2.5. Statistical analysis

After the retrieval of the average pre-processed reflectance spectra from each image partial least squares regression (PLSR) analysis was performed upon the retrieved spectra against the measured moisture content and CIELAB chromatic co-ordinates retrieved from the calibrated RGB images. PLSR analysis was performed upon the normalised and SNV data. PLSR is the most common method for investigating the feasibility of metric prediction in combination with spectroscopy and hyperspectral imagining. It attempts to uncover if any of the retrieved wavelengths vary in a linear manner with respect to the metric investigated. Previous investigations have looked into moisture prediction (ElMasry, Wang, ElSayed, & Ngadi, 2007; Huang, Wang, Zhang, & Zhu, 2014; Pu, Feng, & Sun, 2015), chromaticity (Iqbal, Sun,

& Allen, 2013; Wu, Sun, & He, 2012), maturity (Rajkumar, Wang, EImasry, Raghavan, & Gariepy, 2012) and pH levels (He, Wu, & Sun, 2014) amongst many other metrics.

For the statistical investigations the measured hops were split into the calibration and test sets on a random 2:1 ratio, on the basis of replicate number. Furthermore each model was cross validated for a total of 10 times to ensure all combinations of calibration and test sets were tested.

3. Results and Discussion

The first stage of results is that of the retrieved average spectra for a given batch of hops during the drying process. Figure 7 illustrates the variation in normalised reflectance for the 12kg hop batch dried at 65°C with an air speed of 0.35 m/s.

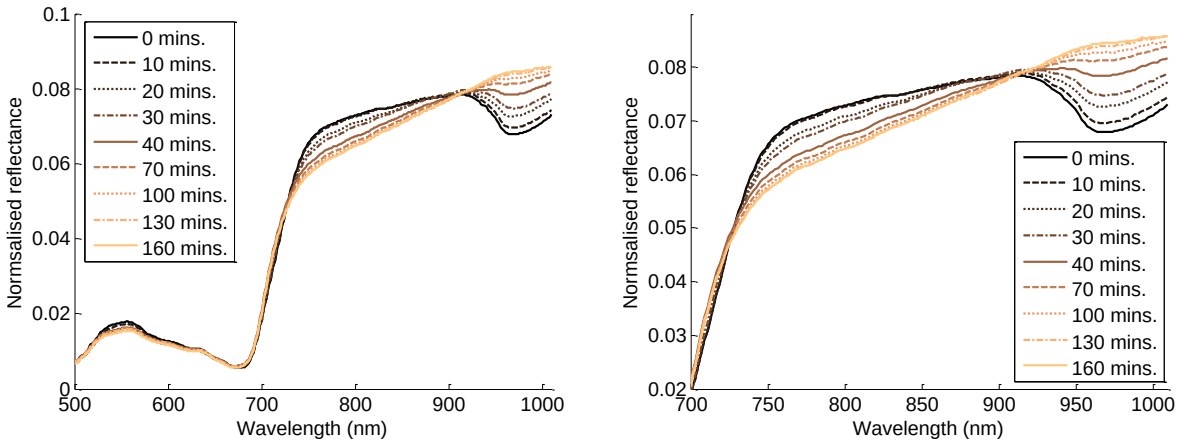

Figure 7. Variation in normalised hop reflectance across a) 500-1010nm, and b) 700-1010nm.

Figure 7a. illustrates the most usable wavelength region from 500 – 1010nm, this is due to the low emission of the halogen light source below 500nm. However it can also be noted that the retrieved reflectance information is greater above 700nm. With this is mind the PLSR analysis was undertaken in the 500-1010nm range. The green peak present at roughly 550nm (Figure 7a.), is reduced in size as drying occurs. Also of great interest is how the peaks and troughs present in the 700-1010nm region are removed as drying occurs. The trough at roughly 970nm is known to be directly related to the third overtone of the O-H bonds within water molecules. Figures 8 and 9 illustrate the changes in moisture content, CIELAB a* and CIELAB b* across the same drying time points for comparison.

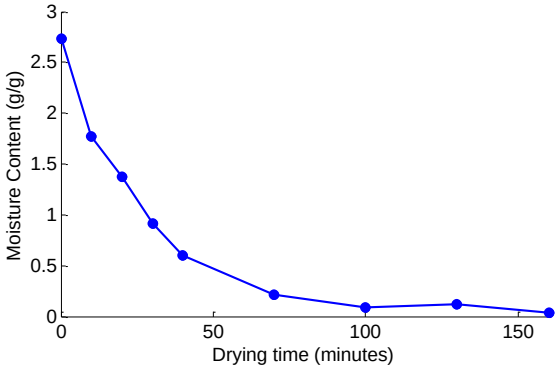

Figure 8. Moisture content change during drying for the hops shown within Figure 8.

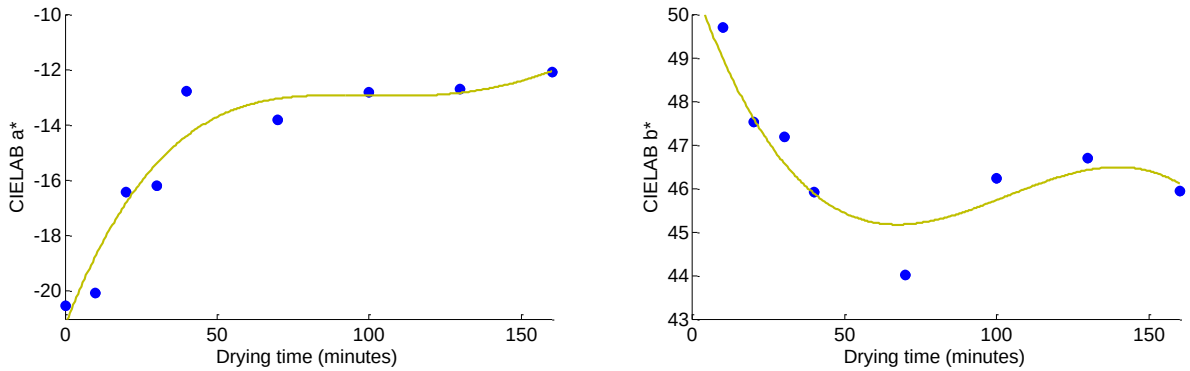

Figure 9. Chromatic changes during drying upon CIELAB a) a*, and b) b* co-ordinates

Table 1. PLSR Results

Pre-processing	Quality Metric	Full Wavelength Set				Reduced Wavelength Set				Wavelengths
		Calibration		Test		Calibration		Test		
		R^2	RMSE	R^2	RMSE	R^2	RMSE	R^2	RMSE	
Normalised	M.C.	1.00	0.05	0.96	0.21	0.96	0.22	0.94	0.27	[508, 697, 741, 768, 814, 844, 918,1000]
	CIELAB a*	0.99	0.62	0.71	3.62	0.89	2.49	0.68	4.08	[501, 697, 753, 768, 793, 827, 966, 985]
	CIELAB b*	0.99	0.47	0.43	2.71	0.75	2.22	0.52	2.66	[507, 714, 753, 822, 928, 1010]
SNV	M.C.	1.00	0.03	0.95	0.24	0.95	0.25	0.91	0.33	[501, 560, 664, 816, 847, 915]
	CIELAB a*	1.00	0.45	0.68	3.97	0.88	2.68	0.75	3.75	[508, 557, 756, 766, 807, 839, 953, 971, 985, 993]
	CIELAB b*	0.99	0.37	0.38	2.90	0.84	1.69	0.37	3.27	[501, 545, 658, 700, 755, 769, 807, 927, 967, 982, 1007]

The results of the models developed above show that basic prediction of hop moisture content and CIELAB chromaticity can indeed be carried out. Moisture content estimation can be carried out to a lower error using the normalised retrieved spectra during drying. This produces a model which uses only 8 wavelengths and achieves a test set r^2=0.94 and RMSE=0.27 in comparison to r^2=0.91 and RMSE=0.33 for the SNV based model (6 wavelengths). This level of performance, when compared to the moisture content change shown in Figure 8, can be seen to be useful up until the last stages of drying. However the consistent RMSE performance between the calibration and test sets for the reduced wavelength set shows the importance of the selected wavelengths. The large variation between the full wavelength set models however does point to a problem with overfitting to the calibration set, which may have been caused by any variation in initial hop quality.

However CIELAB a* prediction can be seen to be better serviced using the SNV spectra with test set results of r^2=0.75 and RMSE=3.75. Whilst for CIELAB b* prediction use of the normalised spectra led to the best performing model with test set performance of r^2=0.52 and RMSE=2.66. Both of these chromaticity prediction models can be seen to not be accurate enough when using Figure 9 as a reference.

The current predictive models are at a usable level of performance, however the possibility to improve them exists. A number of future changes will involve altering the illumination utilised for hyperspectral imaging. This will involve the usage of an illumination which includes a greater output within the blue-green region of electromagnetic space (400-600nm) in an attempt to equalise it. This will give more information for both moisture content and chromatic prediction models. On top of this other spectral pre-processing methods such as use of 1st and 2nd order derivatives in combination to Savitzky-Golay filtering will also be investigated.

4. Conclusions

The work shown here has illustrated the feasibility of moisture content and chromatic information prediction during hop drying using a novel dryer and imaging system. The developed models has shown a level of acceptable performance, with future improvements likely to enhance this further. The design and combination of the hyperspectral and RGB imaging systems within the hop dryer are also noted to be novel and have shown a new manner in which hops can be monitored, in real time, during drying. Future work to improve the predictive models has also been outlined.

Acknowledgements

The Authors give thanks to the University of Kassel for their financial support in the framework of Nachwuchsgruppen program and also to HVG Hopfenverwertungsgenossenschaft e.G..

References

Amigo, J. M., Martí, I., & Gowen, A. (2013). Hyperspectral Imaging and Chemometrics. A Perfect Combination for the Analysis of Food Structure, Composition and Quality. *Data Handling in Science and Technology*, *28*, 343–370. http://doi.org/10.1016/B978-0-444-59528-7.00009-0

Crichton, S., Sturm, B., & Hurlbert, A. (2015). Moisture content measurement in dried apple produce through visible wavelength hyperspectral imaging. In *2015 ASABE Annual International Meeting* (p. 1).

Crichton, S., Shrestha, L., Hurlbert, A., & Sturm, B. (2016), Predicition of moisture content and chromaticity of raw and pre-treated apples slices during convection drying using hyperpsectral imaging. *Journal of Food Engineering* (Submitted)

ElMasry, G., Wang, N., ElSayed, A., & Ngadi, M. (2007). Hyperspectral imaging for nondestructive determination of some quality attributes for strawberry. *Journal of Food Engineering*, *81*, 98–107. http://doi.org/10.1016/j.jfoodeng.2006.10.016

Finlayson, G. D., MacKiewicz, M., & Hurlbert, A. (2015). Color Correction Using Root-Polynomial Regression. *IEEE Transactions on Image Processing*, *24*(5), 1460–1470. http://doi.org/10.1109/TIP.2015.2405336

He, H. J., Wu, D., & Sun, D. W. (2014). Rapid and non-destructive determination of drip loss and pH distribution in farmed Atlantic salmon (Salmo salar) fillets using visible and near-infrared (Vis-NIR) hyperspectral imaging. *Food Chemistry*, *156*, 394–401. http://doi.org/10.1016/j.foodchem.2014.01.118

Huang, M., Wang, Q., Zhang, M., & Zhu, Q. (2014). Prediction of color and moisture content for vegetable soybean during drying using hyperspectral imaging technology. *Journal of Food Engineering*, *128*, 24–30. http://doi.org/10.1016/j.jfoodeng.2013.12.008

Iqbal, A., Sun, D.-W., & Allen, P. (2013). Prediction of moisture, color and pH in cooked, pre-sliced turkey hams by NIR hyperspectral imaging system. *Journal of Food Engineering*, *117*(1), 42–51. http://doi.org/10.1016/j.jfoodeng.2013.02.001

Pu, Y.-Y., Feng, Y.-Z., & Sun, D.-W. (2015). Recent Progress of Hyperspectral Imaging on Quality and Safety Inspection of Fruits and Vegetables: A Review. *Comprehensive Reviews in Food Science and Food Safety*, *00*, n/a–n/a. http://doi.org/10.1111/1541-4337.12123

Pu, Y.-Y., & Sun, D.-W. (2015). Vis–NIR hyperspectral imaging in visualizing moisture distribution of mango slices during microwave-vacuum drying. *Food Chemistry*, *188*, 271–278. http://doi.org/10.1016/j.foodchem.2015.04.120

Rajkumar, P., Wang, N., EImasry, G., Raghavan, G. S. V, & Gariepy, Y. (2012). Studies on banana fruit quality and maturity stages using hyperspectral imaging. *Journal of Food Engineering*, *108*(1), 194–200. http://doi.org/10.1016/j.jfoodeng.2011.05.002

Wu, D., Shi, H., Wang, S., He, Y., Bao, Y., & Liu, K. (2012). Rapid prediction of moisture content of dehydrated prawns using online hyperspectral imaging system. *Analytica Chimica Acta*, *726*, 57–66. http://doi.org/10.1016/j.aca.2012.03.038

Wu, D., Sun, D. W., & He, Y. (2012). Application of long-wave near infrared hyperspectral imaging for measurement of color distribution in salmon fillet. *Innovative Food Science and Emerging Technologies*, *16*, 361–372. http://doi.org/10.1016/j.ifset.2012.08.003

Wu, D., Wang, S., Wang, N., Nie, P., He, Y., Sun, D. W., & Yao, J. (2013). Application of Time Series Hyperspectral Imaging (TS-HSI) for Determining Water Distribution Within Beef and Spectral Kinetic Analysis During Dehydration. *Food and Bioprocess Technology*, *6*, 2943–2958. http://doi.org/10.1007/s11947-012-0928-0